Journal of the Brazilian Society of Mechanical Sciences and Engineering (2019) 41:18
https://doi.org/10.1007/s40430-018-1527-4

TECHNICAL PAPER

Finite element modeling and parametric analysis of a dielectric elastomer thin-walled cylindrical actuator

Lucas A. Garcia[1] · **Marcelo A. Trindade**[1]

Received: 13 March 2018 / Accepted: 1 December 2018 / Published online: 8 December 2018

Abstract
Due to their high energy density, dielectric elastomers have been widely studied over the last decades, in particular, for applications requiring electromechanical actuators. They are commonly designed using thin-walled elastomeric structures, with particularly interesting dielectric properties, that are covered by flexible electrodes in their upper and lower surfaces. Unlike other potential electromechanical materials, such as piezoelectric ceramics, dielectric elastomers may undergo high deformation levels and, thus, present themselves as interesting alternatives for applications that require greater deformations and/or displacements. Nevertheless, in order to profit from this advantage, the design of dielectric elastomer actuators requires predictive models that properly account for both structural and material behavior under high deformations and also electromechanical coupling. The main objective of this work is to present an assessment of existing nonlinear elastic theories well suited to dielectric elastomers that allow to propose a finite element procedure capable of predicting the electromechanical behavior of a plate-type structure. Finite element results are compared to analytical and experimental ones. Then, the procedure is applied to carry out a parametric analysis of a dielectric elastomer cylindrical actuator. The obtained results indicate that the proposed finite element procedure is capable of well representing the actuator operation. It is shown that important deformations and displacements may be obtained with the proposed dielectric elastomer cylindrical actuator, even when subjected to opposing forces, and its performance may be tuned by changing its geometrical properties.

Keywords Dielectric elastomers · Electromechanical actuators · Finite element modeling

1 Introduction

Due to the potentially high energy density and, hence, applicability as electromechanical actuators, dielectric elastomers (DE) have been widely studied over the last two decades. DE actuators are most commonly found in the form of a thin flat plate made of particular elastomers, chosen according to their dielectric properties. This plate is then entirely covered by flexible electrodes in upper and lower surfaces. Therefore, a difference of electric potential (voltage) may be applied to the electrodes, leading to the appearance of opposite electric charges in the upper and lower electrodes. Since the core material between electrodes is flexible (elastomer), the attraction between upper and lower electrodes due to the opposite electric charges generate a through-thickness motion (deformation). That is why a DE actuator acts like a 'deformable capacitor'. Also, since the elastomeric core material is practically incompressible, the contraction in the thickness direction is followed by an expansion (elongation) in the other two planar directions. Depending on the desired application, both thickness and planar expansion/contraction may be used to add functionality to the material/structure [2, 7, 12, 17]. Due to their operation mechanism, such DE actuators are also considered as potential artificial muscles [26].

The functional behavior of such materials allows an applied voltage to be converted into a shape change of a plate-like structure, if it is free, or into an equivalent force applied to a blocking or mechanically coupled device [7, 19]. A similar concept can also be extended to more geometrically complex shapes by properly designing the electric boundary conditions (electrode design) and mechanical coupling with adjacent devices. However, for

Technical Editor: Pedro Manuel Calas Lopes Pacheco, D.Sc.

✉ Marcelo A. Trindade
trindade@sc.usp.br

[1] Department of Mechanical Engineering, São Carlos School of Engineering, University of São Paulo, Av. Trabalhador São-Carlense, 400, São Carlos, SP 13566-590, Brazil

more complex geometries, also more complex modeling procedures may be required to relate actuating voltage with free deformation or equivalent blocked force [18, 23].

Unlike other potential electromechanical materials, such as piezoelectric ceramics, dielectric elastomers may undergo large deformation levels and, thus, present themselves as interesting alternatives for applications that require greater deformations and/or displacements. However, in order to profit from this advantage, the design of dielectric elastomer actuators requires predictive models that properly account for both structural and material behavior under large deformations and also electromechanical coupling. Previous works [15, 19, 38] proposed several well-established theories to represent the expected nonlinear elastic material behavior of dielectric elastomers such as, Neo-Hookean, Mooney-Rivlin, Yeoh, Ogden and others. To account for the electromechanical coupling, most works consider that the applied voltage leads to an equivalent Maxwell stress, that is proportional to the square of the voltage applied to the electrodes and is imposed to the elastomeric core layer.

In the open literature, the most commonly used material for designing dielectric elastomer actuators is an acrylic foam double-sided tape, 3M VHB 4910. However, any elastomeric material with low mechanical stiffness, high maximum strain, high dielectric constant, high electrical breakdown strength, high adhesive strength and good temperature stability properties could be a potential candidate for the design of DE actuators [31]. These requirements imply dealing with high electric voltages and mechanical deformations and, thus, a well-adapted predictive model should take these aspects into account.

The main objective of this work is to present an assessment of existing nonlinear elastic theories well suited to dielectric elastomers that allow to propose a finite element procedure capable of predicting the electromechanical behavior of a plate-type structure. Finite element results are compared to analytical and experimental ones. Indeed, most theoretical studies involving dielectric elastomers consider the use of analytical methods to relate applied voltage with structural deformation. These analytical methods require several simplifying assumptions on the material behavior and are restricted to simpler geometries. Thus, some studies proposed using the finite element method for the prediction of more complex problems. However, due to the complexity of implementing and solving efficiently the nonlinear constitutive relations, most of these studies considered adding features, either mechanical or eletrostatic, to existing commercial FEM softwares, such as COMSOL [3, 14, 34] and ABAQUS [13, 28, 32]. Few others proposed to solve the structural and electrostatic problems separately to reduce computational cost [33]. This work presents a simpler alternative that could be implemented, in principle, on any FEM software since the problem is transformed into a purely mechanical one.

Then, the procedure is applied to carry out a parametric analysis of a dielectric elastomer cylindrical actuator. This particular geometry allows an increase in planar stiffness of the actuator and, thus, may be an interesting design solution for the use of expansion (planar) deformations. Thus, DE cylindrical actuators may be an interesting solution for more important axial (longitudinal) deformations, while withstanding opposing forces, as compared for instance to piezoceramic actuators, and with very fast response, as compared for instance to shape memory materials.

Several previous works discussed modeling, experimental tests and applications of dielectric elastomer cylindrical (tubular) actuators. In terms of modeling and experiments, Son and Goulbourne [35] presented some of the first numerical and experimental results for the dynamic response of DE tubular actuators. Melnikov and Ogden [24] introduced important aspects of modeling of thick- and thin-walled DE tubular actuators, including the presence of axial loads and internal pressures. Bortot [4] presented a discussion on modeling and analysis of the nonlinear dynamic response of thick-walled DE tubular actuators.

In terms of applications, they can be mainly grouped in radial or longitudinal actuation. A potential application for the radial deformations of DE tubular actuators is for active fluidic control, such as in peristaltic and micro pumps [6, 21, 22]. Radial DE actuators were also proposed to detect changes in arterial segments [36]. For improved controlling of internal radius, Cohen [10] proposed stacking/layering several DE tubes. As for longitudinal actuation, modeling and experimental evaluation of DE cylindrical actuators focusing on the axial (longitudinal) actuation was presented in [5]. A more recent use of the longitudinal actuating mechanism was proposed by Chakraborti et al. [9] for refreshable Braille displays. Berselli et al. [3] proposed to combine a cylindrical DE film with series of slender beams to provide a quasi-constant thrust along the entire actuator stroke.

Moreover, several authors studied electrostatic instabilities and bifurcations on DE tubular structures [1, 11, 20]. This is caused by the positive feedback of an applied voltage that leads to a decrease of DE thickness which then leads to an increasing of the electric field yielding further thickness decrease. Although it is not the case in the present study, in extreme cases, this could result in an electrical breakdown.

2 Analytical modeling of dielectric elastomers

In this section, some fundamental aspects on hyperelasticity and electromechanical coupling behavior expected for dielectric elastomers are presented. To assess the available modeling

procedures, an analytical modeling and analysis is performed based on simple dielectric elastomer actuator geometries previously studied in the literature and, for which, there are available experimental results.

2.1 Modeling of DE hyperelastic behavior

Since dielectric elastomer actuators are expected to undergo large deformations, a proper predictive model should be based on nonlinear elasticity. Therefore, unless operating conditions and/or applications require only small strains/stresses, for which linear elastic Hooke's law is sufficient, one should consider nonlinear elastic models.

Over the years, several hyperelastic models are being considered for representing large deformation behavior of elastomers, such as Neo-Hookean [37], Mooney-Rivlin [27], Ogden [29], Yeoh [41] and others. These models fully describe the elastic behavior of a material according to a scalar strain energy function W, from which stress-strain constitutive relations may be derived, such that, for an incompressible material, the Cauchy stress tensor is written as

$$\boldsymbol{\sigma} = -p\mathbf{I} + \frac{\partial W}{\partial \mathbf{F}}\mathbf{F}^{\mathrm{t}}, \tag{1}$$

where W is the strain energy function considered for the material, p is the hydrostatic pressure to guarantee incompressibility, $\mathbf{I}$ is the identity matrix and $\mathbf{F}$ is the deformation gradient tensor. The strain energy function W may be written in terms of the invariants of left Cauchy-Green deformation tensor $\mathbf{B} = \mathbf{F}\mathbf{F}^{\mathrm{t}}$. For an incompressible material, these are

$$\begin{aligned} I_1 &= \mathrm{tr}(\mathbf{B}) = \sum_i \lambda_i^2, \\ I_2 &= (1/2)[\mathrm{tr}(\mathbf{B})^2 - \mathrm{tr}(\mathbf{B}^2)] = \sum_i (1/\lambda_i^2), \\ I_3 &= \det(\mathbf{B}) = \Pi_i \lambda_i^2 = 1, \end{aligned} \tag{2}$$

in which λ_i are the stretch ratios for the unit fibers oriented in the three directions of the coordinate system ($i = 1, 2, 3$). The strain energy functions commonly used for dielectric elastomers are shown in Table 1. The parameters of these material models (G, C_1, C_2, C_3, μ_l, k_l) may be identified through curve-fit methods and uniaxial experiments using a rubber rod. Figure 1 shows the behavior of longitudinal force versus longitudinal stretch ratio curve using four material models with parameters identified from curve-fit to uniaxial experiments. It is noticeable that only Ogden and Yeoh models represent both softening and stiffening behaviors expected for such materials.

Table 1 Strain energy functions for nonlinear elastic material models commonly used for dielectric elastomers

Model	Strain energy function
Neo-Hookean	$W = G(I_1 - 3)$
Mooney-Rivlin	$W = C_1(I_1 - 3) + C_2(I_2 - 3)$
Yeoh	$W = C_1(I_1 - 3) + C_2(I_1 - 3)^2 + C_3(I_1 - 3)^3$
Ogden	$W = \sum_l \mu_l(\lambda_1^{k_l} + \lambda_2^{k_l} + \lambda_3^{k_l} - 3)/k_l$

It is worth noticing that these material models parameters are generally fitted using uniaxial experiments. Nevertheless, in the case of non-unidimensional DE actuators, such as plate-type actuators, where transverse stresses no longer vanish, other experiments should be necessary for the identification of material model parameters [25, 39]. It was shown by Wissler and Mazza [39] that only Yeoh model was capable of satisfactorily representing the 3D response observed in practice for a circular plate actuator when using only parameters identified from a uniaxial experiment. Notice also that rate-dependent deformation is not considered here, but could be using a visco-hyperelastic approach such as the one proposed by Patra and Sahu [30]. Important standards for measuring and identifying dielectric elastomers were recently published in [8].

2.2 Modeling of DE electromechanical coupling

Since the dielectric elastomer behaves as a conformable capacitor, it is possible to quantify the compression due to attraction of opposite electric charges using Maxwell stress σ_m, which represents the mechanical stress that should be applied to the electrodes in order to counterbalance electrostatic attraction forces and, thus, the stress induced in the elastomer. The compressive Maxwell stress may be written

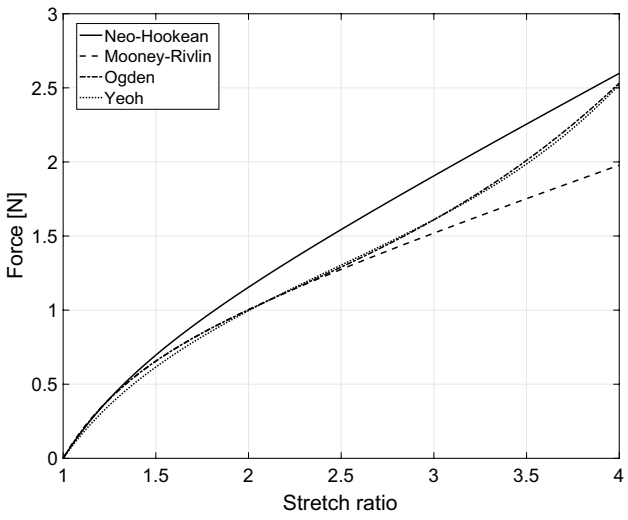

Fig. 1 Comparison between curve-fit of different material models with parameters identified from a uniaxial experiment with a rubber rod

in terms of the electric field acting between the two electrodes (E) and the dielectric stiffness of the elastomer core ($\epsilon_0\epsilon_m$), such that

$$\sigma_m = \epsilon_0\epsilon_m E^2, \tag{3}$$

where ϵ_0 is the dielectric stiffness in the vacuum ($\epsilon_0 = 8.854\ 10^{-12}$ F/m) and ϵ_m is relative dielectric stiffness of the elastomer. Thus, the electromechanical coupling is defined as a nonlinear relation between electric field applied to the electrodes and an equivalent force/stress induced in the dielectric elastomer. If the DE transducer is free, this force will lead to a self-deformation (change in shape) that could serve to a functional purpose. If the DE transducer is mechanically coupled to another structure or device, the equivalent force will be transferred in part to the attached device and, thus, serving as a force actuator.

Considering a uniform electric field between the two parallel electrode plates, such that $E = V/t$, the Maxwell stress may be rewritten in terms of the voltage applied to the electrodes, V, and the distance between electrodes, t, which is also the thickness of DE core. Then,

$$\sigma_m = \epsilon_0\epsilon_m (V/t)^2. \tag{4}$$

Hence, there are three main nonlinear aspects to be considered when modeling dielectric elastomers: (i) the nonlinear elastic behavior and, thus, nonlinear relation between mechanical stress σ_m and stretch ratios λ_i; (ii) the nonlinear relation between mechanical stress σ_m and applied voltage V; and (iii) the nonlinear dependence of mechanical stress σ_m on the thickness t of elastomer core. Hence, whenever a voltage is applied, this leads to a mechanical stress which deforms the elastomer, reducing its thickness following a nonlinear law, which in turn increases the mechanical stress, until equilibrium is reached.

2.3 Analytical results

In this section, a preliminary assessment of the two more accurate proposed models (Ogden and Yeoh) when applied to 3D behavior is performed. For that, a square flat plate made of dielectric elastomer, with thickness 1 mm and length 5 mm, was analyzed. Material parameters obtained by Wissler and Mazza [40] using uniaxial and multi-axial electromechanical tests for VHB 4910 acrylic elastomer are considered: Yeoh model – $C_1 = 82.7$ kPa, $C_2 = -0.747$ kPa, $C_3 = 0.00586$ kPa; Ogden model – $\mu_1 = 8.58$ kPa, $\mu_2 = 84.3$ kPa, $\mu_3 = -23.3$ kPa, $k_1 = 1.293$, $k_2 = 2.3252$, $k_3 = 2.561$. Also, from Kofod [15], the relative dielectric stiffness ϵ_m of VHB 4910 is 4.7.

Considering material isotropy and incompressibility and, also, uniform and equal planar stretch ratios, one may write the transverse (plane) stretch ratios λ_2 and λ_3 in terms of the through-thickness stretch ratio λ_1, such that

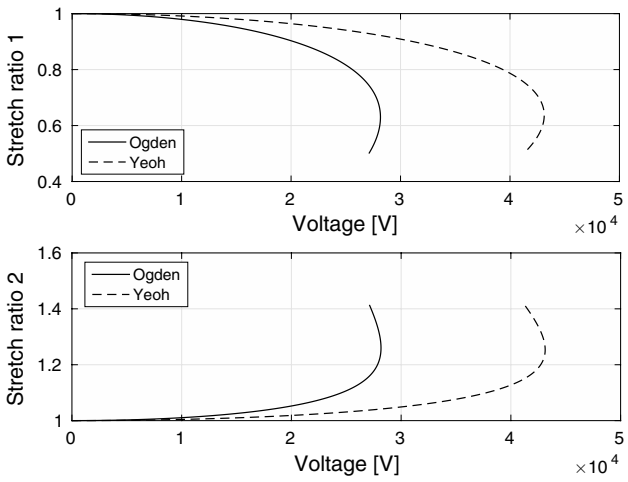

Fig. 2 Stretch ratios versus applied voltage for VHB 4910 square plate using Ogden and Yeoh material models

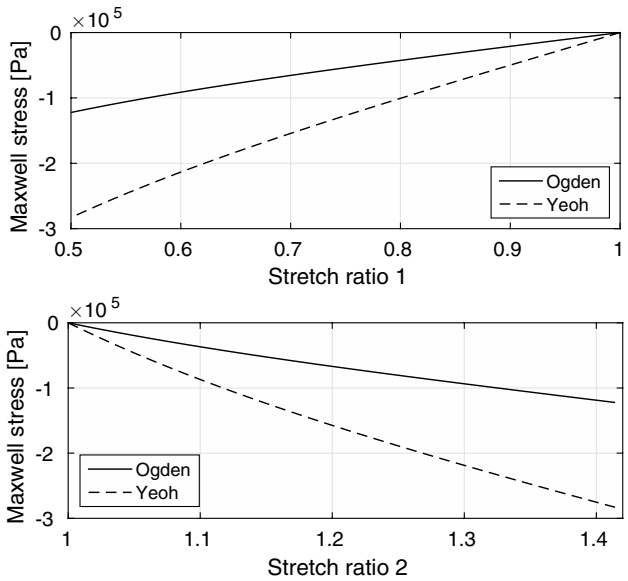

Fig. 3 Stretch ratios versus Maxwell stress for VHB 4910 square plate using Ogden and Yeoh material models

$\lambda_2 = \lambda_3 = 1/\sqrt{\lambda_1}$. Then, choosing a hyperelastic model from Table 1 and using relations (1) and (2), it is possible to evaluate analytically the mechanical stress that would induce a given stretch ratio λ_1. Afterward, using Maxwell stress relation (4), it is also possible to determine the corresponding applied voltage necessary to induce such mechanical stress. This analysis allows to evaluate the relation between applied voltage/stress and through-thickness/planar stretch ratios.

Figures 2 and 3 show the stretch ratios λ_1 and λ_2 versus applied voltage V and Maxwell stress σ_m, respectively,

using Ogden and Yeoh material models. It is possible to observe, in Fig. 2, that an increase in the applied voltage V leads to a through-thickness compression ($\lambda_1 < 1$) accompanied by a planar expansion ($\lambda_2 > 1$) of the plate. However, at some point, it is no longer possible to increase the applied voltage, because further compression would lead to a decrease in the required applied voltage. In fact, after this critical stretch point, the equilibrium is unstable as shown in [16]. Figure 3 shows that the more compressed the material is, the harder to compress it further it becomes. These results show that, for this actuator, it is not possible to obtain planar (lateral) strains larger than 25%, corresponding to a reduction of 44% in the thickness of the actuator. These maximum strains correspond to very different voltages for Ogden (28 kV) and Yeoh (43 kV) models.

3 Finite element modeling of dielectric elastomers

The previous analyses may be quite useful for a preliminary evaluation of mechanical and electromechanical behaviors and potential actuation performance of dielectric elastomers, but they are limited for very simple geometries and uniform deformation assumptions. To enable the study of DE actuators with more complex geometries, a finite element procedure is proposed. For that, ANSYS commercial software was used. First, the hyperelastic behavior was verified using the simple bar geometry considered by Kofod [15] to enable comparison with his experimental results. Then, a verification of the electromechanical behavior using VHB 4910 material models presented previously is performed and the obtained finite element results are compared to the analytical ones.

3.1 Verification of hyperelastic behavior

As a first verification, the experimental test presented by Kofod [15] using a generic rubber was considered to assess the correct representation of the hyperelastic behavior in the finite element model. The bar specimen studied by Kofod [15] had dimensions 1.22 mm × 1.33 mm × 15.7 mm and, in the present work, was modeled in ANSYS using 550 SOLID186 elements. The applied force values were defined to allow coverage of a wide deformation range and 3 equally spaced force sub-steps were considered in the simulation. To deal with the solution of the nonlinear static problem, a modified Newton-Raphson method was used. Figure 4 shows that the results obtained using the finite element model for the relation between force and longitudinal stretch ratio agree very well with the curve-fitted experimental results presented by Kofod [15].

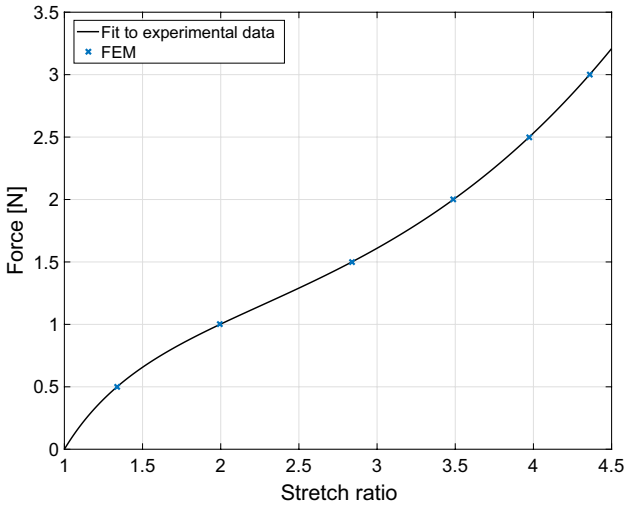

Fig. 4 Force versus longitudinal stretch ratio for rubber bar studied by Kofod [15]

Then, a finite element analysis of the square flat plate made of VHB 4910 dielectric elastomer, studied previously using an analytical modeling, is performed. The material and geometrical properties are the same ones used for the previously presented analytical results. In ANSYS, 75 SOLID186 elements were considered (3 divisions in thickness direction and 5 divisions in the other two directions). In the lower surface, a friction-free in-plane sliding boundary condition was applied, whereas, in the upper surface, a uniform pressure load was considered. The stress versus through-thickness and planar stretch ratios curves obtained using finite element and analytical models are shown in Fig. 5. It is noticeable that FE and analytical models lead to very similar results. In fact, the largest relative differences obtained were 0.6% for Yeoh model and 5.8% for Ogden model. This suggests that Yeoh model might indeed be more adequate for 3D analyses.

3.2 Verification of electromechanical behavior

Then, the electromechanical behavior obtained using the finite element procedure was also verified by comparing with previously presented analytical results. Since a purely mechanical analysis is performed in ANSYS, an iterative method was proposed to relate a desired applied voltage to the corresponding Maxwell stress, which is then applied to the plate using the finite element model in order to evaluate its deformation. A schematic representation of the iterative process is shown in Fig. 6. First, for any given applied voltage V and initial plate thickness t_0, a corresponding compressive Maxwell stress σ_0 is evaluated and applied as a mechanical loading condition to the plate. This leads to a compression of the plate, resulting in a decrease of its thickness to t_1. For this reason, with the same applied voltage, the

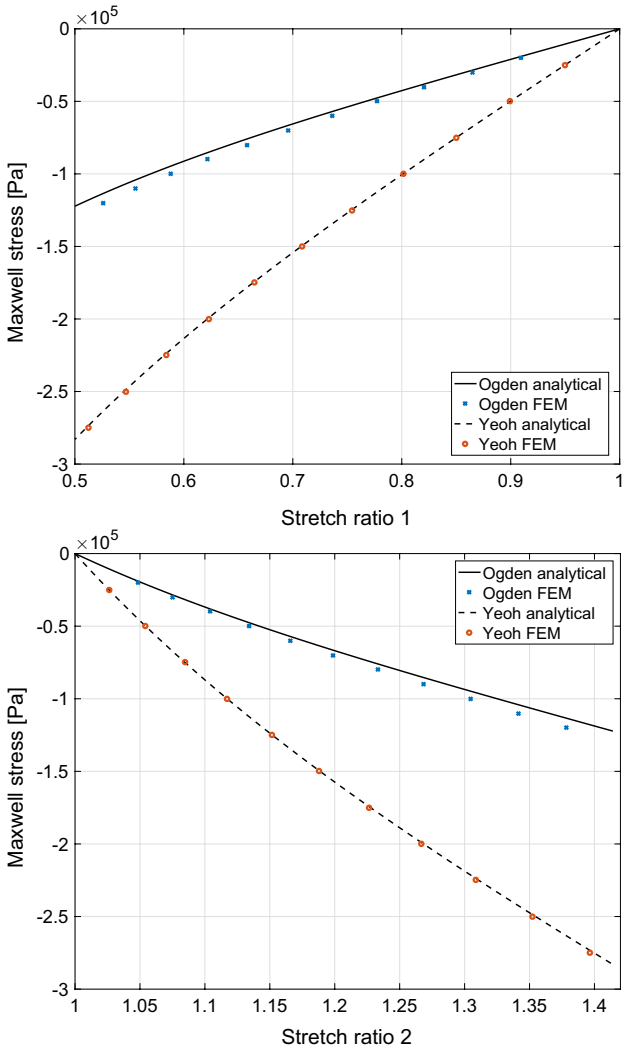

Fig. 5 Stress versus through-thickness and planar stretch ratios using finite element and analytical models

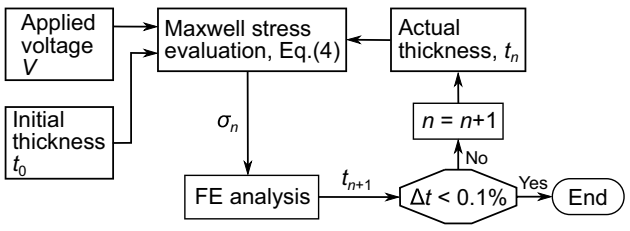

Fig. 6 Finite element scheme for calculation of deformed configuration due to applied voltage

Maxwell stress is modified (increased) to σ_1, which is again applied to the plate, leading to an even smaller thickness t_2. This iterative process continues until the plate thickness converges within a threshold (relative difference between iterations of 0.1%). The process is then repeated for every value of applied voltage V. For each simulation, the same procedure used in previous analyses for the solution of the nonlinear elastic static problem was considered.

Figure 7 shows the electromechanical behavior represented by the applied voltage versus through-thickness stretch ratio curves obtained using finite element and analytical models and considering Ogden and Yeoh material models. Similarly to the purely mechanical analysis, the difference between analytical and finite element results are smaller for Yeoh material model. For Ogden material model, the relative differences are of approximately 5%. It is also worthwhile to mention that the iterative method stops converging for higher values of applied voltage, confirming the limiting voltages for the dielectric elastomers presented previously.

4 Parametric analysis of dielectric elastomer cylindrical actuator

Using the finite element procedure presented previously, a parametric analysis of a dielectric elastomer thin-walled cylindrical actuator, schematically represented in Fig. 8, is performed. The initial dimensions are: thickness $t = 0.6$ mm, diameter $2R = 20$ mm, length $L = 20$ mm. The actuator is made of 3M VHB 4910 dielectric elastomer fully covered by electrodes in the inner and outer surfaces. The hyperelastic material behavior is represented using Yeoh model with previously presented parameters.

In a first analysis, it is desired to study the axial (lengthwise or heightwise) deformation of the actuator when it is subjected to an applied voltage. This is done for two sets of mechanical boundary conditions: in the first case, the actuator is free to move and, in the second case, the actuator

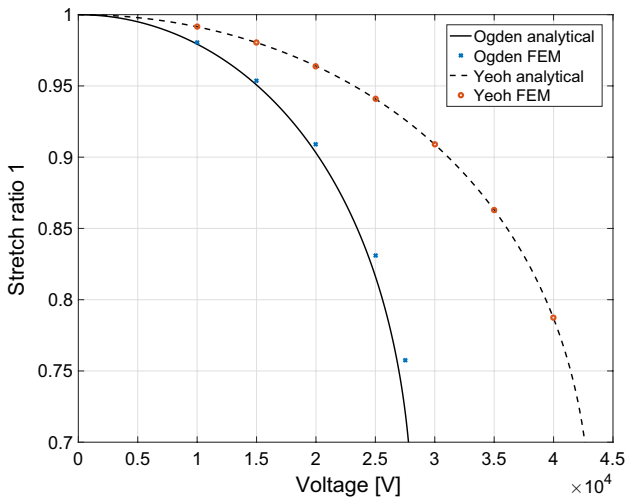

Fig. 7 Applied voltage versus through-thickness stretch ratio using finite element and analytical models

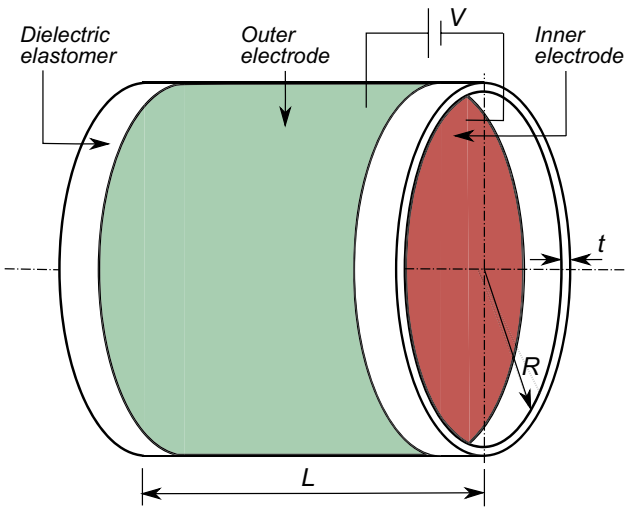

Fig. 8 Schematic representation of the thin-walled cylindrical actuator made of dielectric elastomer

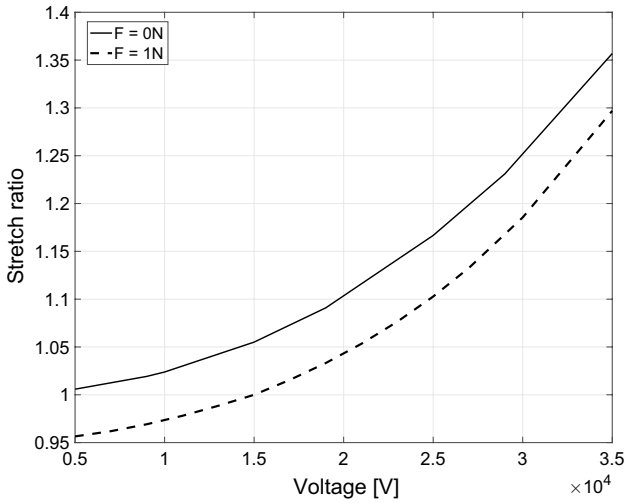

Fig. 9 Lengthwise stretch ratio versus applied voltage for a DE thin-walled cylindrical actuator

is also subjected to an axial mechanical force opposing to the axial displacement (semi-free or semi-blocked). To save computational effort, a bidimensional axisymmetric finite element model is built in ANSYS, using 114 PLANE183 elements. For that, the boundary conditions were defined as: the cylinder symmetry axis is not allowed to move, the cylinder base is always in the same plane (friction-free sliding), opposite pressures (Maxwell stress) are applied at the inner and outer surfaces, and a compressive mechanical force $F = 1$ N in the axial direction may be applied at the free end of the cylinder (in semi-blocked case).

Figure 9 presents the lengthwise stretch ratio versus applied voltage for the thin-walled cylindrical actuator. It is noticeable that the presence of a compressive mechanical force (F) leads to an offset in the stretch ratio, such that 15 kV are necessary to counterbalance the through-length compression. But, in both cases, reasonable stretch ratios can be obtained, leading to an increase of 30% (with compressive force of 1 N), 6 mm, to 35% (free), 7 mm, in cylinder length. This length increase is accompanied by a reduction in cylinder wall thickness and diameter. Figure 10 shows the deformed configuration of the cylinder for maximum applied voltage, 35 kV, where only half cylinder is shown for better visualization.

Then, a parametric analysis is performed to evaluate the effect of two geometric parameters, thickness and diameter, on the actuator response. For that, a single loading condition was considered, with applied voltage of 20 kV and compressive mechanical force of 1 N. First, the cylinder wall thickness was varied between 0.4 and 1 mm, while maintaining the diameter in 20 mm. Results shown in Fig. 11 indicate that smaller thicknesses lead to higher lengthwise stretch ratios, which seems reasonable since increasing thickness values yields smaller actuating electric fields and stiffer cylinders.

Next, the cylinder diameter was varied between 8 and 60 mm, while maintaining the wall thickness in 0.5 mm. Figure 12 presents the obtained stretch ratios for increasing values of cylinder diameter. One may notice that higher diameters seem more interesting for providing higher lengthwise stretch ratios, although for diameters larger than 35 mm, further increases in diameter affect less the stretch ratio. Notice, however, that higher diameters and lower wall thicknesses also decrease the buckling stiffness of the cylinder. Therefore, for much higher compressive forces, this aspect should also be accounted for.

5 Conclusions

This work has presented recent results on the modeling and analysis of dielectric elastomer actuators, focusing on: the choice and characterization of well-adapted hyperelastic material models; finite element modeling and analysis procedures for a sample plate dielectric elastomer; and a parametric analysis of a thin-walled cylindrical actuator made of dielectric elastomer. Presented results indicate that the finite element procedure was able to capture the main aspects of actuator operation while being more interesting than analytical modeling for complex geometries. Considering the geometric and material properties assumed here, the dielectric elastomer cylindrical actuator is able to induce important deformations even when subjected to an opposing mechanical force. Future works are being directed to the extension of the proposed methodology for the analysis of other geometric configurations and loading conditions.

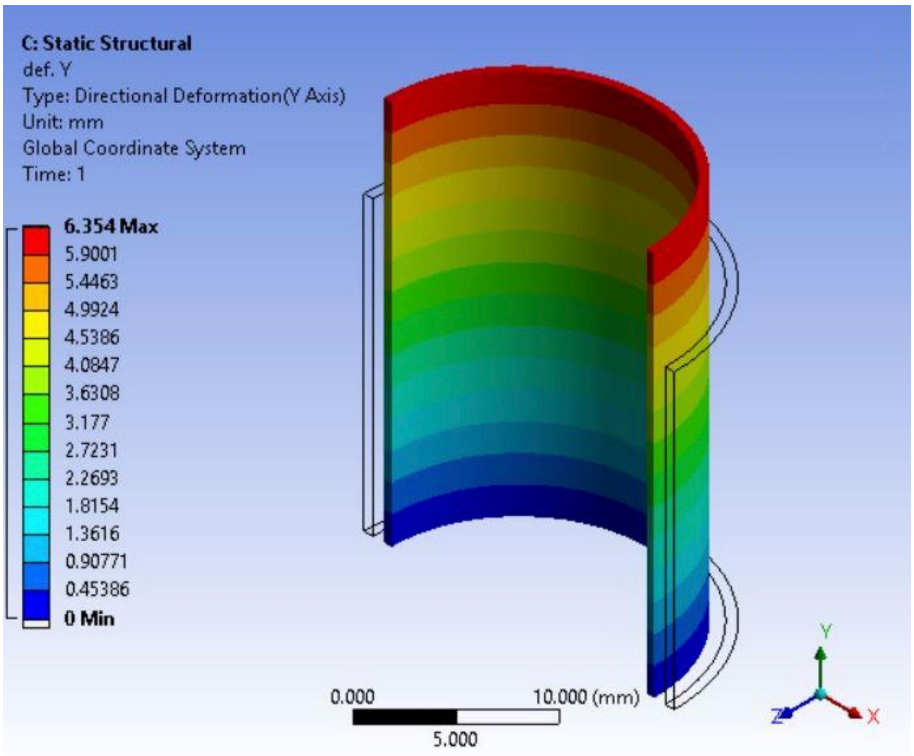

Fig. 10 Deformed configuration due to applied voltage of a DE thin-walled cylindrical actuator

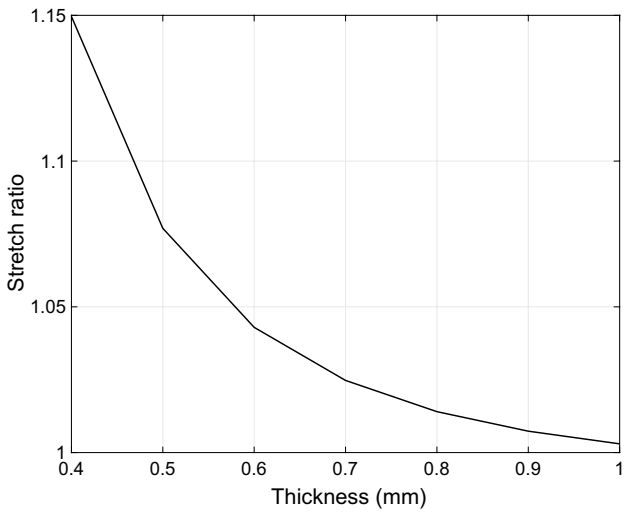

Fig. 11 Lengthwise stretch ratio versus initial thickness of a DE thin-walled cylindrical actuator

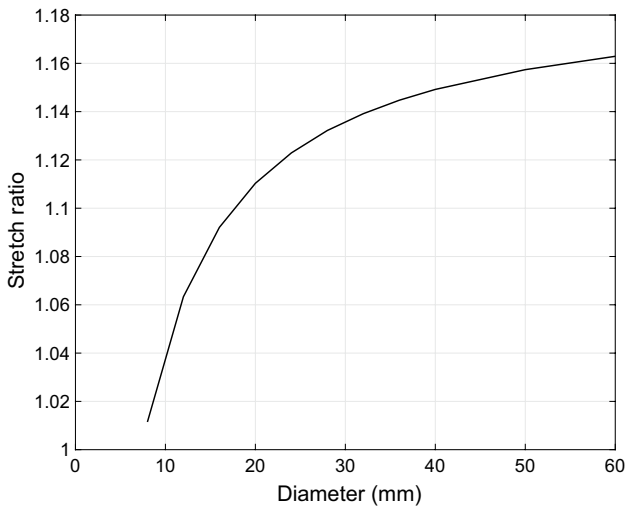

Fig. 12 Lengthwise stretch ratio versus initial diameter of a DE thin-walled cylindrical actuator

Acknowledgements Financial support of National Council for Scientific and Technological Development (CNPq), Grants 574001/2008-5 and 309193/2014-1, and São Paulo Research Foundation (FAPESP), Grant 2016/06511-5, is gratefully acknowledged.

References

1. An L, Wang F, Cheng S, Lu T, Wang TJ (2015) Experimental investigation of the electromechanical phase transition in a dielectric elastomer tube. Smart Mater Struct 24:035006
2. Bar-Cohen Y (2004) Electroactive polymer (EAP) actuators as artificial muscles: reality, potential and challenges, 2nd edn. SPIE Press, Bellingham

3. Berselli G, Mammano GS, Dragoni E (2014) Design of a dielectric elastomer cylindrical actuator with quasi-constant available thrust: modeling procedure and experimental validation. J Mech Des 136:125001
4. Bortot E (2018) Nonlinear dynamic response of soft thick-walled electro-active tubes. Smart Mater Struct 27:105025
5. Carpi F, De Rossi D (2004) Dielectric elastomer cylindrical actuators: electromechanical modelling and experimental evaluation. Mater Sci Eng C 24:555–562
6. Carpi F, Menon C, De Rossi D (2010) Electroactive elastomeric actuator for all-polymer linear peristaltic pumps. IEEE/ASME Trans Mech 15(3):460–470
7. Carpi F, De Rossi D, Kornbluh R, Pelrine R, Sommer-Larsen P (2007) Dielectric elastomers as electromechanical transducers: fundamentals, materials, devices, models and applications of an emerging electroactive polymer technology. Elsevier, Amsterdam
8. Carpi F et al (2015) Standards for dielectric elastomer transducers. Smart Mater Struct 24:105025
9. Chakraborti P, Karahan Toprakci HA, Yang P, Di Spigna N, Franzon P, Ghosh TA (2012) compact dielectric elastomer tubular actuator for refreshable Braille displays. Sens Actuators A Phys 179:151–157
10. Cohen N (2017) Stacked dielectric tubes with electromechanically controlled radii. Int J Solids Struct 108:40–48
11. Díaz-Calleja R, Sanchis MJ, Riande E (2010) Instability of incompressible cylinder rubber tubes under radial electric fields. Eur Phys J E 32:183–190
12. Dorfmann L, Ogden RW (2018) The effect of deformation dependent permittivity on the elastic response of a finitely deformed dielectric tube. Mech Res Commun 93:47–57
13. Foo CC, Zhang Z-Q (2015) A finite element method for inhomogeneous deformation of viscoelastic dielectric elastomers. Int J Appl Mech 7(5):1550069
14. Jia K, Lu T (2016) Numerical study on the electromechanical behavior of dielectric elastomer with the influence of surrounding medium. Int J Smart and Nano Mater 7(1):52–68
15. Kofod G (2001) Dielectric elastomer actuators. Ph.D. Thesis, Riso National Laboratory
16. Kofod G, Sommer-Larsen P (2008) Finite elasticity models of actuation. In: Carpi F et al (ed) Dielectric elastomers as electromechanical transducers: fundamentals, materials, devices, models and applications of an emerging electroactive polymer technology. Elsevier Science, Amsterdam, pp 159–168
17. Lampani L, Gaudenzi P (2010) 3D finite element analyses of multilayer dielectric elastomer actuators with metallic compliant electrodes for space applications. J Intell Mater Syst Struct 21:621–632
18. Liu J, Foo CC, Zhang Z-Q (2017) A 3D multi-field element for simulating the electromechanical coupling behavior of dielectric elastomers. Acta Mech Solida Sin 30:374–389
19. Lochmatter P (2007) Development of a shell-like electroactive polymer (EAP) actuator. Ph.D. Thesis, ETH Zurich
20. Lu T, An L, Li J, Yuan C, Wang TJ (2015) Electro-mechanical coupling bifurcation and bulging propagation in a cylindrical dielectric elastomer tube. J Mech Phys Solids 85:160–175
21. Mao G, Wu L, Fu Y, Chen Z, Natani S, Gou Z, Ruan X, Qu S (2018) Design and characterization of a soft dielectric elastomer peristaltic pump driven by electromechanical load. IEEE/ASME Trans Mech 23(5):2132–2143
22. McCoul D, Pei Q (2015) Tubular dielectric elastomer actuator for active fluidic control. Smart Mater Struct 24:105016
23. McGough K, Ahmed S, Frecker M, Ounaies Z (2014) Finite element analysis and validation of dielectric elastomer actuators used for active origami. Smart Mater Struct 23:094002
24. Melnikov A, Ogden RW (2016) Finite deformations of an electroelastic circular cylindrical tube. Zeitschrift für Angewandte Mathematik und Physik (ZAMP) 67:140
25. Meunier L, Chagnon G, Favier D, Orgéas L, Vacher P (2008) Mechanical experimental characterisation and numerical modeling of an unfilled silicone rubber. Polym Test 27:765–777
26. Mirkavili SM, Hunter IW (2018) Artificial muscles: mechanisms, applications and challenges. Adv Mater 30:1704407
27. Mooney M (1940) A theory of large elastic deformation. J Appl Phys 11:582–592
28. O'Brien B, McKay T, Calius E, Xie S, Anderson I (2009) Finite element modelling of dielectric elastomer minimum energy structures. Appl Phys A Mater Sci Process 94:507–514
29. Ogden R (1972) Large deformation isotropic elasticity on the correlation of theory and experiment for incompressible rubberlike solids. Proc R Soc Lond A 326:565–584
30. Patra K, Sahu RK (2015) A visco-hyperelastic approach to modelling rate-dependent large deformation of a dielectric acrylic elastomer. Int J Mech Mater Des 11:79–90
31. Pelrine R, Kornbluh R, Pei Q, Joseph J (2000) High-speed electrically actuated elastomers with strain greater than 100%. Science 287(5454):836–839
32. Qu S, Suo Z (2012) A finite element method for dielectric elastomer transducers. Acta Mech Sol Sin 25(5):459–466
33. Seifi S, Park KC, Park HS (2018) A staggered explicit-implicit finite element formulation for electroactive polymers. Comput Method Appl Mech Eng 337:150–164
34. Simone F, Linnebach P, Rizzello G, Seelecke S (2018) A finite element model of rigid body structures actuated by dielectric elastomer actuators. Smart Mater Struct 27:065001
35. Son S, Goulbourne NC (2010) Dynamic response of tubular dielectric elastomer transducers. Int J Solids Struct 47:2672–2679
36. Son S, Goulbourne NC (2012) Large strain analysis of a soft polymer electromechanical sensor coupled to an arterial segment. J Intell Mater Syst Struct 23(5):575–586
37. Treloar LRG (1943) The elasticity of a network of long chain molecules II. Trans Faraday Soc 39(9–10):241–246
38. Wissler M (2007) Modeling dielectric elastomer actuators. Ph.D. Thesis, ETH Zurich
39. Wissler M, Mazza E (2005) Modeling and simulation of dielectric elastomer actuators. Smart Mater Struct 14:1396–1402
40. Wissler M, Mazza E (2007) Mechanical behavior of an acrylic elastomer used in dielectric elastomer actuators. Sens Actuators A 134:494–504
41. Yeoh OH (1990) Characterization of elastic properties of carbon-black-filled rubber vulcanizates. Rubber Chem Technol 63(5):792–805